Proton Irradiation Effects on Resistive Random Access Memory With ZrO$_X$/HfO$_X$ Stacks

Daeseok Lee, Joonmyoung Lee, Seungjae Jung, Seonghyun Kim, Jubong Park, K. P. Biju, Minhyeok Choe, Takhee Lee, and Hyunsang Hwang

Abstract—In this study, we investigated proton irradiation effects on resistive random access memory (ReRAM) comprising ZrO$_x$/HfO$_x$ stacks. After irradiation, changes of current were observed in the initial state (IS). From the electrical conduction mechanism in the IS, we have concluded that the different initial conditions of the active layer lead to different radiation effects. The radiation-induced leakage paths have been concluded as main origin of the increased leakage current, whereas radiation-induced charge trapping is dominant fact of the decreased leakage current in the IS. From the results of noise analysis in the low resistance state (LRS) and high resistance state (HRS), we observed that the radiation effects became negligible because of the formed local conducting path during forming process.

Index Terms—Low frequency noise, proton, radiation effect, ReRAM.

I. INTRODUCTION

RECENTLY, resistive random access memory (ReRAM) has been extensively studied for application in next-generation nonvolatile memory devices owing to its advantages such as low power consumption, fast switching speed, and capacitor-like simple design [1], [2]. In addition, ReRAM has been considered to be a promising candidate for use in aerospace applications or other radiation environments because of its switching mechanism which is reversible resistive switching behavior. Considering the fact that irradiation induce various damages on performance of charge control memories, the resistive switching memory could be one of promising device for the radiation environment applications [3]–[6]. However, there have been only few studies about the effects of radiation on ReRAM, despite the fact that ionizing radiation can lead some degradations such as displacement damage, nuclear reaction, radiation-induced leakage current (RILC),

radiation-induced soft/hard breakdown (RSB/RHB), and radiation-induced charge trapping on dielectric layers [7]–[12]. In this study, a ReRAM device with ZrO$_x$/HfO$_x$ stacks was exposed to proton irradiation to investigate the effects of radiation on the device. The radiation effects were studied by a low frequency noise (LFN) analysis (which is highly sensitive to traps and can offer additional significant information regarding the electrical characteristics of devices) [13]–[15].

II. EXPERIMENT

ReRAM devices composed of ZrO$_x$/HfO$_x$ stacks with an active area of 50×50 μm^2 were fabricated. The 3-nm-thick HfO$_x$ layer was deposited as an active layer on a TiN substrate by atomic layer deposition. As a top electrode, Zr/Pt layers were subsequently deposited under optimized conditions by reactive sputtering. In this structure, the Zr layer was considered as a metallic layer, which can play a role of oxygen reservoir. The fabrication process is described in more detail elsewhere [16]. To investigate radiation effects, we have compared irradiated samples with unirradiated samples. To prepare the irradiated samples, a high-energy proton beam was incident on the as-fabricated ReRAM devices (irradiation time $= 6000$ s, beam energy $= 10$ MeV, fluence $= 10^{12}$ cm^{-2}, and absorbed dose $= 6.41 \times 10^6$ rad). The electrical properties of the devices were evaluated by an Agilent 4155A semiconductor parameter analyzer. For better understanding, a noise analysis was performed by a SR570 low-noise current amplifier and an Agilent 35670A dynamic signal analyzer. To achieve more reliable results in noise analysis, we used normalized and averaged sufficient data (several times in one cell and cell-to-cell).

III. RESULTS

The ZrO$_x$/HfO$_x$ bi-layered ReRAM shows bi-polar memory switching behavior, as shown in Fig. 1. The initial state (IS) is changed to a low-resistance state (LRS) under positive bias, which can be considered as the first electrical soft break down, known as forming process in binary oxides RRAM applications [17], [18]. Continuously, the LRS is changed to a high-resistance state (HRS), when a negative bias is applied; this polarity dependent switching makes our device bi-polar instead of unipolar (polarity independent). The HRS is changed to LRS again under a lower positive voltage than that of the first dielectric soft break down voltage or forming voltage. The resistance changes under applied bias are called respectively as FORMING process, RESET process, and SET process. This device shows the set and forming process only under a positive bias, while the reset process occurs under a negative bias. After this first switching cycle (from forming process to set process),

Fig. 1. Typical current-voltage (I-V) properties of unirradiated sample. The arrows having numbers mean switching sequences. The first change from IS to LRS is named as forming process (no. 1). The state is changed from LRS to HRS by applying negative bias (no. 2), while HRS is changed to LRS under positive bias (no. 3). After the first cycle ($1 \rightarrow 2 \rightarrow 3$), this device follows the memory switching ($2 \rightarrow 3$).
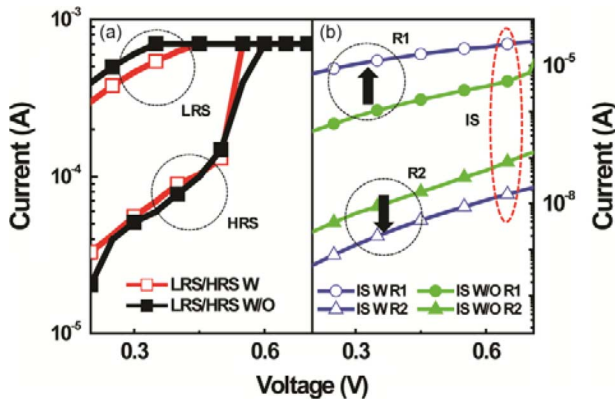
Fig. 2. Comparing I-V properties of both irradiated and unirradiated samples. (a) Similar current values of both irradiated and unirradiated samples were observed in LRS and HRS, (b) while the irradiated samples showed current changes in the IS. The changes in the irradiated samples are named as R1 (change-result 1) and R2 (change-result 2).

the device shows consecutive memory switching, i.e., changes in state at around 0.8 V and -1.3 V. According to previous studies about switching mechanism, these resistance changes can be explained as the redox reaction at the top interface. Under the positive bias, the oxygen in the HfO_x layer moves upward direction to Zr layer, and then the metallic Zr layer is oxidized. As the oxygen ions move upward direction, conducting oxygen vacancies move downward direction and thus form local conducting path. Consequently, the state is changed to LRS. Conversely, during reset process, the oxygen which is absorbed in Zr layer is released and further oxidizes the conducting path which is composed of the conducting oxygen vacancies. Finally, the LRS is changed to HRS, and shows successive memory switching [19], [16].

The Fig. 2 shows current-voltage (I-V) curves of irradiated and unirradiated samples in HRS, LRS (a), and IS (b). The irradiated samples showed changes in the IS, whereas similar values of current were observed in the LRS and HRS. These results indicate that the radiation effects became negligible by the formation of conducting path during forming process. To verify the formation of conducting path, the noise analysis was performed.
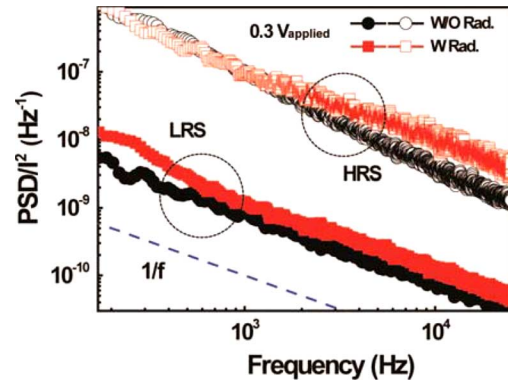
Fig. 3. Noise measurement results for both irradiated and unirradiated samples in LRS and HRS. The results of both samples showed similar values in each state (LRS, HRS) respectively.
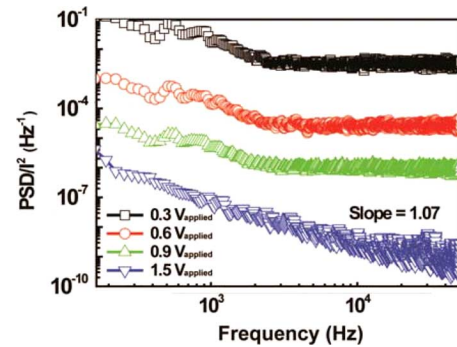
Fig. 4. Noise measurement results under various applied voltages. The PSD values decreased as applied bias increased. Under the 1.5 $V_{applied}$ biasing, the PSD showed 1/f noise, which indicates the formation of local conducting path.

Fig. 3 shows average power spectral densities (PSDs) in LRS and HRS for both irradiated and unirradiated samples. In both states, the PSDs showed the conventional 1/f noise shape and showed similar values. The higher value of PSD in HRS can be explained as influence of traps, as described in previous studies [19], [20]. These results (the similar value of PSD in LRS and HRS) also support that the radiation effects which lead changes in the IS become negligible after the forming process. Moreover, the formation of local conducting path during forming process was confirmed by applying various applied voltages, as shown in Fig. 4. The average PSDs of unirradiated sample showed resistor noise behavior (which comprises 1/f noise and thermal noise) under 0.3, 0.6, and 0.9 $V_{applied}$ [21]. The PSDs are decreased as the applied voltage increased, then under $V_{applied} = 1.5$ V (near forming voltage), the shape of PSD was clearly changed to shape of 1/f noise with a slope of 1.07. As the applied voltage increased, the decrease of resistance leads to decrease of thermal noise, which is proportional to the resistance [21]. In other words, these results confirm that the local conducting path was formed at 1.5 $V_{applied}$, and then the local conducting path led to the decrease of resistance and thermal noise. Consequently, the shape of PSD was changed from resistor noise to 1/f noise. In addition, the 1/f noise without the thermal noise under 1.5 $V_{applied}$ showed similar value with PSD of HRS. It is also correlated with the formation of the conducting path. From
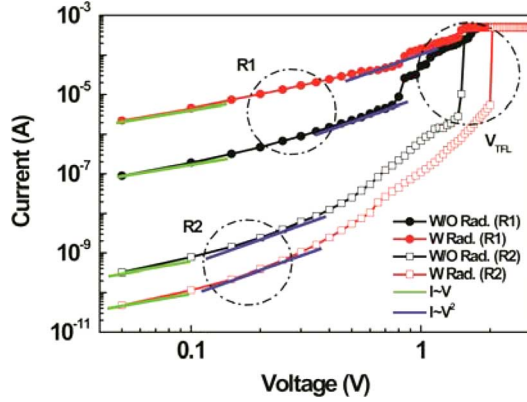
Fig. 5. Log I—Log V plots of both irradiated and unirradiated samples in the IS. The curves are well fitted according to the space-charge-limited current (SCLC) theory. Only the R2 case (decreased current behavior) showed the SCLC having exponentially distributed trap energy. These results clearly support that the different initial conditions of HfO$_x$ can lead different radiation effects in the IS.

these results, we have concluded that the radiation effects became negligible by the formation of conducting path. Considering the fact that the most current in LRS and HRS flow through the local conducting path unlike the IS current flow, we speculate that the radiation effects in oxide layer could be a minor factor during current flow after forming process.

On the other hand, some changes are observed in the IS, as shown in Fig. 2(b). Notice that the Fig. 2(b) shows I-V curves in IS for both irradiated and unirradiated samples. The observed changes of irradiated samples can be divided into change-result 1 (R1) and change-result 2 (R2). We named the increased current behavior and the reduced current behavior as R1 and R2, respectively. These different results indicate that the irradiation caused opposite effects in R1 and R2. To investigate the different tendencies in more detail, the electrical conduction mechanism in the IS was studied, as shown in Fig. 5. The log-I and log-V plots are fitted to explain the space-charge-limited current (SCLC) in this device. According to the SCLC theory, under low voltage, I-V curve shows the ohmic behavior (I∼V) with the slope 1. It is because of the domination of the thermally generated free carriers as compared with the injected charge carriers. After the ohmic region, the slopes are changed to 2, which are generally explained as the trap-associated SCLC. Finally, the current was abruptly changed at the forming voltages. This voltage can be considered as the trap-filled limit voltage (V$_{TFL}$). However, only for the case R2, the plots showed steeper slopes after the trap-associated SCLC. It can be considered as the SCLC with exponentially distributed trap energy. These results clearly show that the initial conditions of active layers are different [22].

The current of IS was increased in R1, whereas that was decreased in R2. These results indicate that the different initial conditions of the active layer leads to different radiation effects in the IS. Even though the radiation can generate various kinds of traps such as hydrogen motion associated defects in specific case, charged traps, and leakage paths in oxide layer, the radiation induced leakage paths can be dominantly generated in R1
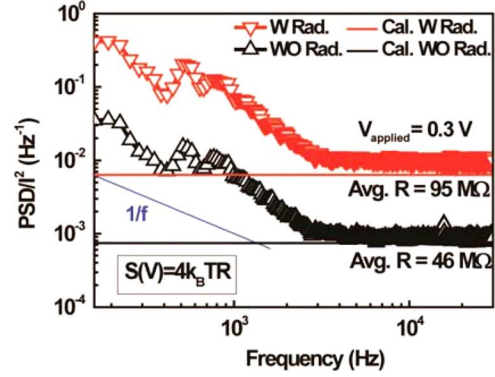
Fig. 6. Noise analysis results with the calculated thermal noise value for deeper understanding about radiation effects in R2. Both of irradiated and unirradiated samples showed resistor noise behavior and the PSD value of irradiated samples was higher than that of the unirradiated samples.
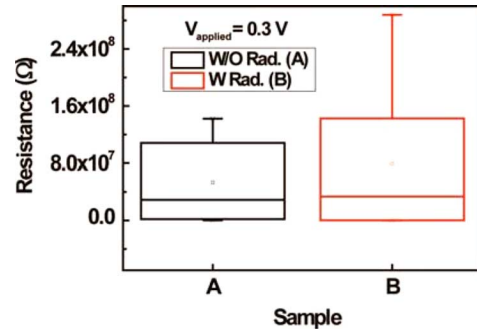
Fig. 7. Statistical device-to-device resistance distribution. The irradiated samples showed less stable distribution of resistance, which means the less stable electric characteristics of device.

[7]–[12], [23], [24]. The fact that the IS current value of R1 is similar with the current value of HRS is also related with the radiation effect of R1. Contrary to the result of R1, the decreased current in R2 can result from the radiation induced charged traps. To achieve better understanding, noise analysis was performed for R2. Fig. 6 shows the measured PSDs of R2 for both irradiated and unirradiated samples. To compare these values, normalization was carried out. The measured PSDs showed the resistor noise behavior which has excess noise (1/f noise shape) and thermal noise. According to the fact that excess noise has 1/f noise shape and values depend on the fabrication process, the 1/f noise line was used to indicate the excess noise for easier understanding. Moreover, the thermal noise was derived by

$$S(V) = 4K_B TR$$

where K_B is the Boltzmann's constant, T is temperature, and R is the average resistance of results showed in Fig. 7 (statistical device-to-device resistance distribution) [21]. The excess noises of measured PSDs showed the similar slope of 1/f noise. Furthermore, the thermal noises of measured PSDs were similar with the calculated thermal noise values for both of the samples. The PSD value of irradiated samples was one order of magnitude higher than that of the unirradiated samples. These results show that the PSDs can be considered as the resistor noise and

the resistance of irradiated samples is increased by the irradiation. Considering the fact that proton irradiation can generate charged traps in oxide layers, those results can come from the radiation-induced charge trapping. Moreover, an increased distribution of resistance in R2 was observed, which implies that electrical characteristics of the irradiated devices became less stable and not uniform, as shown in Fig. 7.

IV. CONCLUSIONS AND DISCUSSION

In conclusion, the proton irradiation effects on ReRAM having ZrO_x/HfO_x stacks were observed in the IS. The changes were increased current behavior and decreased current behavior. From the analysis of electrical conduction mechanism, we have concluded that the different initial condition of active layer leads to different radiation effects in IS. The main reason of the increased current behavior was concluded as the radiation-induced leakage paths in the oxide layer. From the noise analysis of the decreased current behavior case, radiation-induced charge trapping was considered as the dominant factor. Moreover, the observed radiation effects of the IS became negligible after the forming process, due to the formation of local conducting path in active layer. The formation of conducting path verified by noise analysis was the determining factor in overcoming the radiation effects.

REFERENCES

[1] R. Waser and M. Aono, "Nanoionics-based resistive switching memories," *Nature Mater.*, vol. 6, pp. 833–840, Nov. 2007.

[2] C. Cen, S. Thiel, J. Mannhart, and J. Levy, "Oxide nanoelectronics on demand," *Science*, vol. 323, no. 5917, pp. 1026–1030, Feb. 2009.

[3] C. Claeys, H. Ohyama, E. Simoen, M. Nakabayashi, and K. Kobayashi, "Radiation damage in flash memory cells," *Nucl. Instrum. Methods Phys. Res. B*, vol. 186, pp. 392–400, 2002.

[4] D. N. Nguyen, C. I. Lee, and A. H. Johnston, "Total ionizing dose effects on flash memories," in *Proc. IEEE Radiation Effects Data Workshop Rec.*, 1998, pp. 100–103.

[5] D. F. Sampson, "Time and total dose response of non-volatile uvproms," *IEEE Trans. Nucl. Sci.*, vol. 35, no. 6, pp. 1542–1546, Dec. 1988.

[6] W. Wester, C. Nelson, and J. Marriner, "Proton irradiation effects on 2 Gb flash memory," in *Proc. IEEE Radiation Effects Data Workshop Rec.*, 2004, pp. 68–71.

[7] J. R. Srour, C. J. Marshall, and P. W. Marshall, "Review of displacement damage effects in silicon devices," *IEEE Trans. Nucl. Sci.*, vol. 50, no. 3, pp. 653–670, Jun. 2003.

[8] A. Paccagnella, A. Candelori, A. Milani, E. Formigoni, G. Ghidini, F. Pellizzer, D. Drera, P. G. Fuochi, and M. Lavale, "Breakdown properties of irradiated MOS capacitors," *IEEE Trans. Nucl. Sci.*, vol. 43, no. 6, pp. 2609–2616, Dec. 1996.

[9] A. H. Johnston, G. M. Swift, T. Miyahira, and L. D. Edmonds, "Breakdown of gate oxides during irradiation with heavy ions," *IEEE Trans. Nucl. Sci.*, vol. 45, no. 6, pp. 2500–2508, Dec. 1998.

[10] B. Butcher, X. He, M. Huang, Y. Wang, Q. Liu, H. Lv, M. Liu, and W. Wang, "Proton-based total-dose irradiation effects on Cu/Hf_{O2}: Cu/PtReRAM devices," *Nanotech.*, vol. 21, no. 47, p. 475206, Nov. 2010.

[11] T. P. Ma and P. V. Dressendorfer, *Ionizing Radiation Effects in MOS Devices and Circuits*.   New York: Wiley, 1989.

[12] B. Miao, R. Mahapatra, R. Jenkins, J. Silvie, N. G. Wright, and A. B. Horsfall, "Radiation induced change in defect density in HfO_2-based MIM capacitors," *IEEE Trans. Nucl. Sci.*, vol. 56, no. 5, pp. 2916–2924, Oct. 2009.

[13] L. K. J. Vandamme and F. N. Hooge, "What do we certainly know about 1/f noise in MOSTs?," *IEEE Trans. Electron Devices*, vol. 55, no. 11, pp. 3070–3085, Nov. 2008.

[14] D. M. Fleetwood, T. L. Meisenheimer, and J. H. Scofield, "1/f noise and radiation effects in MOS devices," *IEEE Trans. Electron Devices*, vol. 41, pp. 1953–1964, Nov. 1994.

[15] J.-K. Lee, H. Y. Jeong, I.-T. Cho, J. Y. Lee, S.-Y. Choi, H.-I. Kwon, and J.-H. Lee, "Conduction and low-frequency noise analysis in Al/α-TiO_x/Al bipolar switching resistance random access memory devices," *IEEE Electron Device Lett.*, vol. 31, no. 6, pp. 603–605, Apr. 2010.

[16] J. M. Lee, E. M. Bourim, W. T. Lee, J. B. Park, M. S. Jo, S. J. Jung, J. H. Shin, and H. S. Hwang, "Effect of ZrO_x/HfO_x bilayer structure on switching uniformity and reliability in nonvolatile memory applications," *Appl. Phys. Lett.*, vol. 97, p. 172105, Oct. 2010.

[17] K. Fujiwara, T. Nemoto, M. J. Rozenberg, Y. Nakamura, and H. Takagi, "Resistance switching and formation of a conductive bridge in metal/binary oxide/metal structure for memory devices," *Jpn. J. Appl. Phys.*, vol. 47, no. 8, p. 6266, Aug. 2008.

[18] D. S. Lee, H. Choi, H. Sim, D. Choi, H. Hwang, M. Lee, S. Seo, and I. Yoo, "Resistance switching of the nonstoichiometric Zirconium oxide for nonvolatile memory applications," *IEEE Electron Device Lett.*, vol. 26, no. 9, pp. 719–721, Oct. 2005.

[19] D. Lee, J. Lee, M. Jo, J. Park, M. Siddik, and H. Hwang, "Noise-analysis-based model of filamentary switching ReRAM with ZrO_x/HfO_x stacks," *IEEE Electron Device Lett.*, vol. 32, no. 7, pp. 964–966, Jul. 2011.

[20] J. Lee, J. Shin, D. Lee, W. Lee, S. Jung, M. Jo, J. Park, K. P. Biju, S. Kim, S. Park, and H. Hwang, "Diode-less nano-scale ZrO_x/HfO_x RRAM device with excellent switching uniformity and reliability for high-density cross-point memory applications," *IEDM Tech. Dig.*, pp. 452–455, Dec. 2010.

[21] G. Vasilescu, *Electronic Noise and Interfering Signals*.   Heidelberg, Germany: Springer, 2005.

[22] Y. Kim, S.-I. Ohmi, K. Tsutsui, and H. Iwai, "Space-charge-limited currents in La_2O_3 thin films deposited by E-beam evaporation after low temperature dry-nitrogen annealing," *Jpn. J. Appl. Phys.*, vol. 44, no. 6A, p. 4032, Jun. 2005.

[23] X. J. Zhou, D. M. Fleetwood, L. Tsetseris, R. D. Schrimpf, and S. T. Pantelides, "Effects of switched-bias annealing on charge trapping in HfO_2 gate dielectrics," *IEEE Trans. Nucl. Sci.*, vol. 53, no. 6, pp. 3636–3643, Dec. 2006.

[24] A. G. Marinopoulos, I. Batyrev, X. J. Zhou, R. D. Schrimpf, D. M. Fleetwood, and S. T. Pantelides, "Hydrogen shuttling near Hf-defect complexes in $Si/SiO_2/HfO_2$ structures," *Appl. Phys. Lett.*, vol. 91, pp. 233–503, Dec. 2007.